Available online at www.sciencedirect.com

ScienceDirect

Journal of the Chinese Institute of Chemical Engineers 38 (2007) 409–418

JOURNAL OF THE CHINESE INSTITUTE OF CHEMICAL ENGINEERS

www.elsevier.com/locate/jcice

Drag on two co-axial rigid spheres moving normal to a plane: Newtonian and Carreau fluids

Jyh-Ping Hsu [1,*], Shu-Chuan Yang [2], Jung-Chieh Chen [3]

Department of Chemical Engineering, National Taiwan University, Taipei 10617, Taiwan

Received 11 April 2007; accepted 29 June 2007

Abstract

The boundary effect and the presence of a nearby entity on the drag of a rigid entity is investigated by considering the movement of two identical, rigid, coaxial spheres normal to a plane in both a Newtonian and a Carreau fluid at a low to medium large Reynolds number. The parameters key to the phenomenon under consideration, including the nature of the fluid, the separation distance between two spheres, the distance between the near sphere and the plane, and the Reynolds number, on the drag coefficient are discussed. We show that the influence of a boundary on the drag coefficient is more important than that of the nature of a fluid and that of the separation distance between two spheres. The variation of the drag coefficient as a function of Reynolds number for a Carreau fluid is similar to that for a Newtonian fluid. Due to the shear-thinning nature of the former the drag coefficient in the former is smaller than that in the latter. The influence of the index parameter of a Carreau fluid becomes appreciable only if the Carreau number is sufficiently large. Correlations between the drag coefficient and the key parameters of a system are developed for the case when the Reynolds number is smaller than l.

Keywords: Sedimentation; Boundary effect; Two coaxial rigid spheres normal to a plane; Newtonian and Carreau fluid; Drag coefficient

1. Introduction

Evaluation of the drag on a particle as it moves in a fluid medium is a classic problem, and is of both fundamental and industrial importance.

Sedimentation, which is often adopted to estimate the physical properties of a particle and is a typical unit operation in water and wastewater treatment, for example, involves this problem. Although both experimental and theoretical results are ample in the literature, the drag on a particle under general conditions has not been reported, and relevant investigations remain active. The difficulty involved depends largely on the degree of complexity of the associated flow field, which is related to the geometry of a particle, the nature of fluid medium, and the level of Reynolds number. In practice, the influence of neighboring particles and that of a boundary also need be considered. These factors are usually taking into account by a correction factor, which is a function of the Reynolds number, the size and the geometry of a particle, and its relative position and distance from a boundary.

For non-Newtonian fluids, the problem becomes even more complicated since the viscosity could be position dependent. Several attempts have been made to investigate the sedimentation of an isolated particle in a non-Newtonian fluid. Rodrigue *et al*. (1996), for instance, studied the behaviors of both rigid spheres and bubbles in an infinite Carreau fluid under creeping flow conditions. Adachi *et al*. (1973) examined the behavior of a sphere in a shear-thinning fluid by partitioning the drag into a friction term and a pressure term. The former increases with the increase in the degree of the shear-thinning nature of a fluid, but the reverse is true for the latter. Ceylan *et al*. (1999) evaluated the drag on a rigid sphere in a power law fluid for the case when the Reynolds number is lower than 1000 and the power law index ranges from 0.5 to 1.0. Adopting a finite element method, Tripathi and Chhabra (1995) simulated the relation between the drag coefficient and the Reynolds number for both spheres and spheroids in a power-law fluid having shear-thickening nature. Missirlis *et al*. (2001) discussed the influence of a boundary on the drag on a rigid sphere by considering a sphere in a cylinder filled with a power-law fluid having shear-thinning nature at a low Reynolds number. Kelessidis and Mpandelis (2004) observed the sedimentation of a spherical particle in a

* Corresponding author. Fax: +886 2 23623040.
E-mail address: jphsu@ntu.edu.tw (J.-P. Hsu).
[1] 徐治平
[2] 楊淑娟
[3] 陳榮傑

0368-1653/$ – see front matter © 2007 Taiwan Institute of Chemical Engineers. Published by Elsevier B.V. All rights reserved.
doi:10.1016/j.jcice.2007.06.005

Nomenclature

A_n	projection area of a particle on a plane normal to its motion (m^2)
C_D	drag coefficient
Cu	Carreau number ($=2\lambda u_t/d$)
D	diameter of a sphere (m)
$\overline{\overline{D}}$	deformation tensor
F_D	drag (kg m/s^2)
h	distance between the center of near sphere and plane (m)
h_c	critical distance (m)
n	power law index
P	pressure (kg/m s^2)
r	radius of a sphere (m)
S	center-to-center distance between two spheres (m)
T	transpose of matrix
Re	Reynolds number ($=\rho u_t d/\eta$)
$\mathbf{u}$	fluid velocity (m/s)
u_t	bounded terminal velocity of a particle (m/s)
u_x	fluid velocity in x-direction (m/s)
x, y, z	Cartesian coordinates (m)

Greek symbols

$\dot{\gamma}$	magnitude of shear rate tensor (1/s)
η	viscosity of fluid (kg/m s)
η_0	zero shear rate viscosity (kg/m s)
η_∞	infinite shear rate viscosity (kg/m s)
λ	relaxation time constant (s)
μ	viscosity of Newtonian fluid (kg/m s)
ρ	density of fluid (kg/m^3)
$\overline{\overline{\tau}}$	shear rate tensor (kg/m s^2)

Mathematical symbols

∇	gradient operator (1/m)
$\nabla\bullet$	divergence operator (1/m)

power-law fluid having shear-thinning nature. A correlation relation between the drag coefficient and the Reynolds number was proposed for the Reynolds number in the range [0.1,1000]. Machač *et al.* studied the sedimentation of spherical (2000) and non-spherical particles (2002) in a Carreau fluid at a low Reynolds number. In a study of the sedimentation of a rigid sphere in a Carreau fluid Chhabra and Uhlherr (1980) reported an empirical expression, which correlates the drag coefficient with the Reynolds number and the key parameters of a Carreau fluid. Based on a reciprocal theorem, Becker *et al.* (1996) investigated the sedimentation of a rigid sphere near a planar wall. Both Newtonian fluid and an elastic fluid having shear-thinning nature were considered.

In this study the effects of the presence of a boundary and neighboring particles and the nature of fluid medium on the behavior of a rigid sphere is investigated by considering two identical, coaxial spheres moving normal to a plane, both in a Newtonian and in a shear-thinning Carreau fluid. The flow field is solved numerically based on a finite element scheme and the influences of the key parameters of the system under consideration, including the separation distance between two spheres, the distance between a sphere and a plane, the Reynolds number, and the properties of a fluid, on the drag coefficient of a sphere are discussed.

2. Theory

Referring to Fig. 1, we consider the moving of two identical, rigid, coaxial spheres of radius r and diameter D normal to a plane with constant velocity u_t. Let h be the distance between the center of the near sphere and the plane and S be the center-to-center distance between two spheres. The coordinates (x, y, z) with its origin located at the centerline of system are adopted. For convenience, both spheres are fixed in the space and the plane and the fluid moving with a relative velocity u_t in the reverse direction. Suppose that the fluid is incompressible. Then the flow field can be described by

$$\nabla \cdot \mathbf{u} = 0 \tag{1}$$

$$\rho \mathbf{u} \cdot \nabla \mathbf{u} = -\nabla P + \nabla \cdot \overline{\overline{\boldsymbol{\tau}}} \tag{2}$$

where ρ is the density of fluid, $\mathbf{u}$ is the fluid velocity, ∇ is the gradient operator, P is the modified pressure which includes the gravitational effect, $\overline{\overline{\boldsymbol{\tau}}}$ is the shear rate tensor, and

$$\nabla \mathbf{u} = \frac{1}{2}[\nabla \mathbf{u} + (\nabla \mathbf{u})^{\mathrm{T}}] = \frac{1}{2}\overline{\overline{\mathbf{D}}} \tag{3}$$

$$\overline{\overline{\boldsymbol{\tau}}} = -\eta(\overline{\overline{\mathbf{D}}})\overline{\overline{\mathbf{D}}} = -\eta(\overline{\overline{\mathbf{D}}})(\nabla \mathbf{u} + (\nabla \mathbf{u})^{\mathrm{T}}) \tag{4}$$

In these expressions, $\eta(\overline{\overline{\mathbf{D}}})$ is the apparent viscosity, $\overline{\overline{\mathbf{D}}}$ the deformation tensor, and T denotes matrix transpose. $\eta(\overline{\overline{\mathbf{D}}})$ can be transformed into a scalar function $\eta(\dot{\gamma})$ through

$$\dot{\gamma} = \sqrt{\frac{1}{2}(\overline{\overline{\mathbf{D}}} : \overline{\overline{\mathbf{D}}})} \tag{5}$$

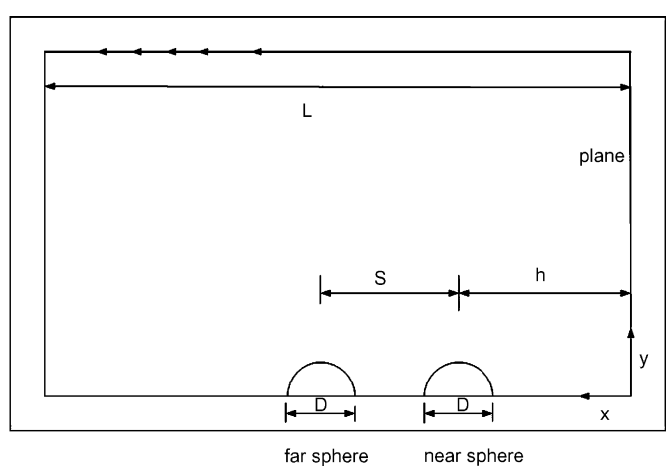

Fig. 1. Schematic representation of the problem considered, where two identical, coaxial, rigid spheres of radius r and diameter D moving normal to a plane, h is the distance between the center of the near sphere and the plane, and S is the center-to-center distance between the two spheres. The coordinates (x, y, z) with its origin located at the centerline of the system are adopted.

where $\dot{\gamma}$ is the shear rate, which is a function of the nature of a fluid. For the present Carreau fluid, we assume (Machač *et al.*, 2000)

$$\eta(\dot{\gamma}) = \eta_0[1 + (\lambda\dot{\gamma})^2]^{(n-1)/2} \tag{6}$$

where η_0 is the viscosity at zero shear rate, λ is the relaxation time constant, and n is the power law index. Note that a Newtonian fluid is a special case of the present Carreau fluid with $n = 1$ or $\lambda = 0$.

The present problem is of two-dimensional nature, and the boundary conditions associated with Eqs. (1) and (2) are assumed as

$$u_x = u_t, u_y = 0 \text{ as } x \to \infty \tag{7}$$

$$u_x = u_t, u_y = 0 \text{ as } y \to \infty \tag{8}$$

$$u_x = 0,\ u_y = 0 \text{ on particle surface} \tag{9}$$

$$\frac{\partial u_x}{\partial y} = 0,\ y = 0 \tag{10}$$

Eq. (9) describes the no-slip nature of the particle surface, and Eq. (10) arises from the symmetric nature of the present system.

The governing equations for the flow field and the associated boundary conditions are solved numerically by FIDAP, a commercial software based on Galerkins' weighted residuals method. Double precision is used throughout the computation, and grid independence is checked to ensure that the mesh used is fine enough. The number of meshes used is on the order of 10,000, and the tolerance is on the level of 3%. The applicability of this software is justified by comparing the results obtained with the corresponding analytical results of Happel and Brenner (1983) for both a rigid sphere moving normal to a plane in a Newtonian fluid and two identical rigid spheres in an unbound Newtonian fluid. Fig. 2 and Table 1 reveal that the performance of the numerical approach adopted is satisfactory for $Re \leq 0.1$.

3. Results and discussion

Both Newtonian and Carreau fluids are considered in the numerical simulations. For illustration, we assume $\rho = 1000$ kg/m^3 and $\eta_0 = 0.4$ kg/m s in subsequent discussion.

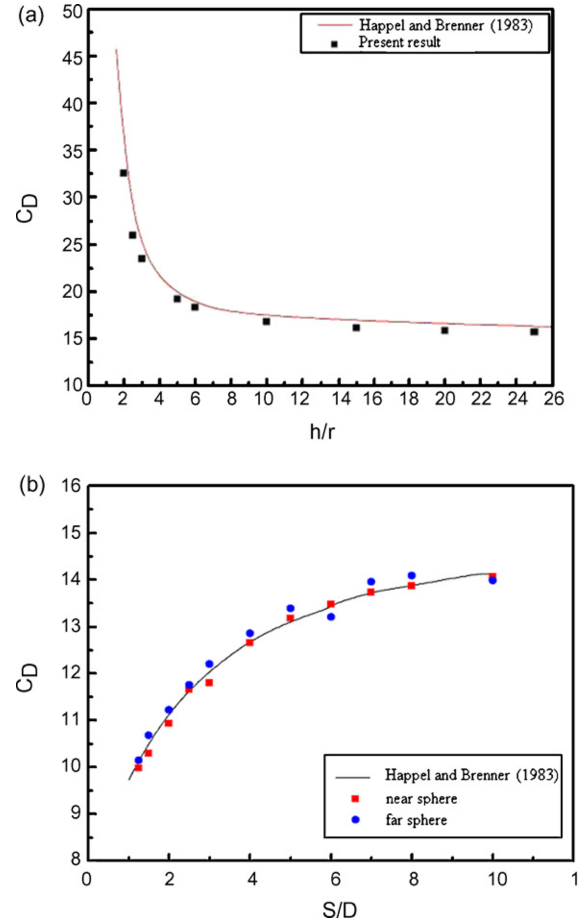

Fig. 2. (a) Variation of C_D as a function of (h/r) for a single sphere moving normal to a plane. (- - -): Analytical result of Happel and Brenner (1983); (■): present result. (b) Variation of C_D as a function of (S/D) for two identical rigid spheres in an unbounded fluid. (—): Analytical result of Happel and Brenner (1983); (■) and (●): present result for the far and near spheres, respectively.

3.1. Newtonian fluid

The variation of C_D as a function of the Reynolds number Re in a Newtonian fluid for various (h/r)s at a fixed (S/D) is illustrated in Fig. 3(a), and that for various (S/D)s at a fixed (h/r) is illustrated in Fig. 3(b). Fig. 3(a) reveals that for both spheres, C_D decreases with the increase in Re, the closer a sphere to a plane the larger is the C_D, and for a fixed Re, the C_D of the near

Table 1
Variation of drag on spheres 1 and 2, F_1 and F_2, respectively, for two rigid spheres in an unbounded Newtonian fluid for various (S/D)s at $Re = 0.1$

S/D	$F_1 \times 10^5$ (analytical)	$F_1 \times 10^5$ (numerical)	Percentage deviation (%)	$F_2 \times 10^5$ (numerical)	Percentage deviation (%)
1.25	10.1514	9.9791	1.6966	10.1490	0.0231
1.5	10.5362	10.3968	1.3226	10.8472	−2.9519
2	11.1913	11.1581	0.2967	11.3957	−1.8262
2.5	11.7157	11.6569	0.5017	11.7545	−0.3310
3	12.1335	11.9961	1.1327	12.4443	−2.5612
4	12.7327	12.6525	0.6296	12.8522	−0.9382
5	13.1305	13.1756	−0.3432	13.3912	−1.9851
6	13.4277	13.4730	−0.3377	13.2060	1.6508
7	13.6843	13.7331	−0.3567	13.9585	−2.0040
8	13.9195	13.8737	0.3290	14.0900	−1.2252
10	14.1985	14.0655	0.9369	13.9855	1.5004

Analytical: Happel and Brenner (1983), F_1(analytical) = F_2(analytical); numerical: present approach.

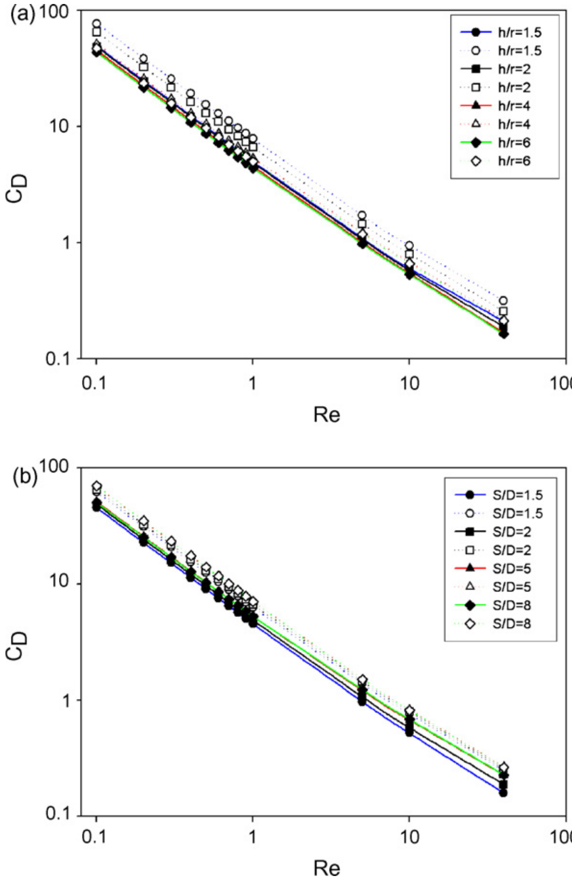

Fig. 3. Variation of C_D as a function of Re in a Newtonian fluid for various (h/r)s at $S/D = 2$, (a), that for various values of (S/D) at $h/r = 2$, (b). Dashed curves: near sphere; solid curves: far sphere.

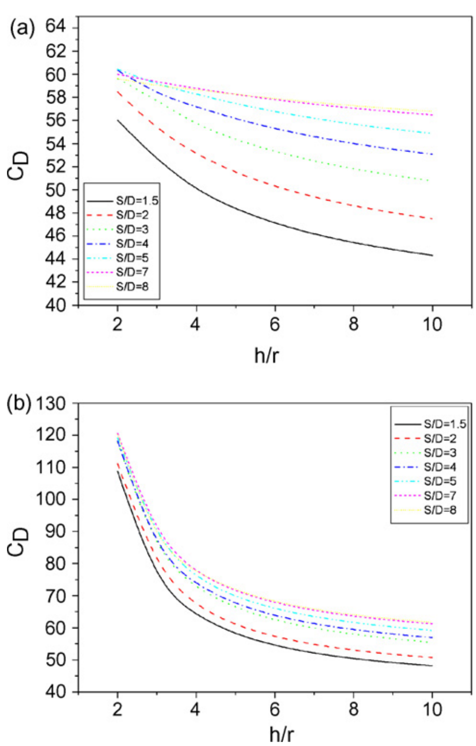

Fig. 4. Variation of C_D as a function of (S/D) in a Newtonian fluid for various (h/r)s at $Re = 0.1$. (a) Far sphere, (b) near sphere.

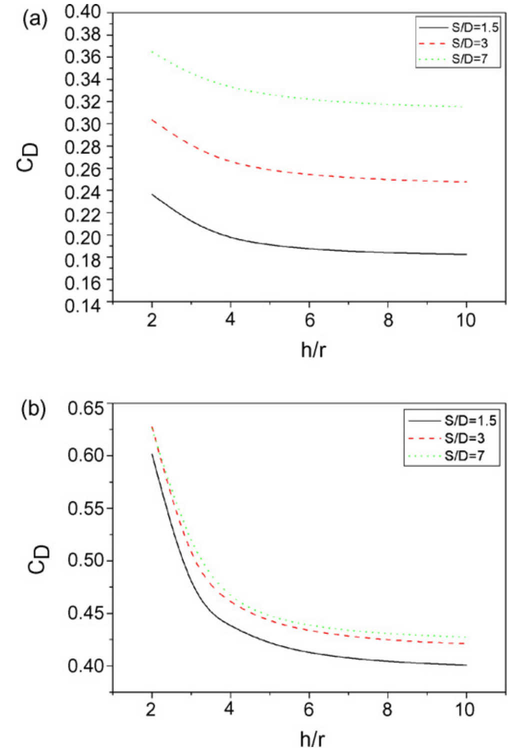

Fig. 5. Variation of C_D as a function of (S/D) in a Newtonian fluid for various (h/r)s at $Re = 40$. (a) Far sphere, (b) near sphere.

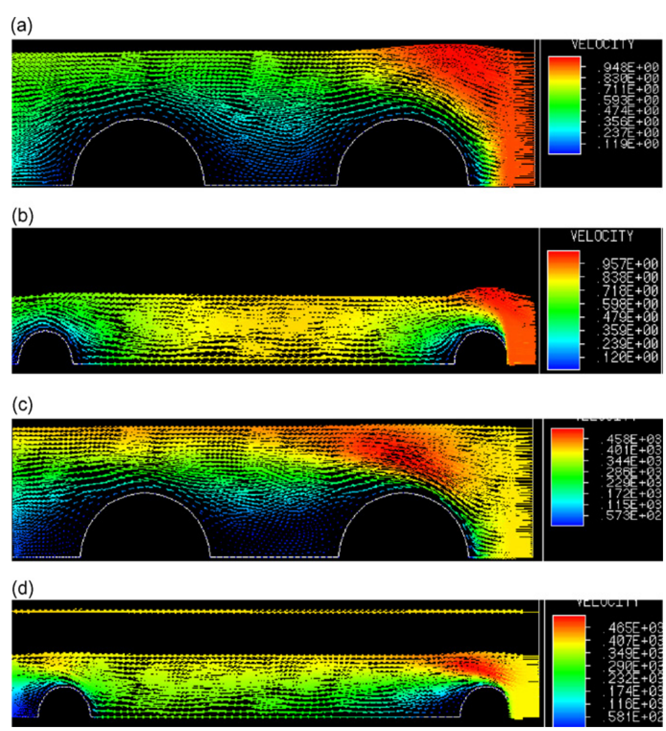

Fig. 6. Some typical flow fields for the cases of Figs. 4 and 5. (a) $S/D = 2$ and $Re = 0.1$, (b) $S/D = 8$ and $Re = 0.1$, (c) $S/D = 2$ and $Re = 40$, (b) $S/D = 8$ and $Re = 40$.

sphere is larger than that of the far sphere. These are because the slower the fluid velocity the greater the drag acting on a sphere. When a sphere is near a plane, the reflection of the local flow filed yields the formation of vortexes, and the net fluid velocity declines. Also, the influence of the plane on the near sphere is more appreciable than that on the far sphere. The drag coefficient of a sphere, C_D, can be defined by $C_D = f/[(\rho u^2/2)(\pi r^2)]$, where f is the drag force acting on the sphere, r is its radius, and u is the magnitude of $\mathbf{u}$. Fig. 3(a) also indicates that if Re is sufficiently small, Stokes law, that is,

$$C_D = \frac{24\mu}{\rho u_t D} = \frac{24}{Re} \quad (11)$$

is applicable to both spheres. A positive deviation from the Stokes law is observed when Re becomes large. Furthermore, the more significant the boundary effect is the smaller the Re at which the deviation occurs. When the far sphere is close to the near sphere, the compression of the wakes between two spheres leads to a decrease in the form drag on the near sphere and an increase in the local Re, and C_D declines accordingly. On the other hand, when the far sphere is away from the near sphere, the interaction between two spheres is lessened, and C_D increases accordingly. If the plane is absent and Re is low, both spheres have the same C_D. When the plane is present, since its influence on the near sphere is more important than that on the far sphere, the C_D of the near sphere is larger than that of the far sphere. If the plane is absent and Re is high, the C_D for the near (leading) sphere is larger than that of the far (rear) sphere. Note that since (h/r) is fixed, an increase in (S/D) implies that the influence of the far sphere on the near sphere declines, but that of the plane on the near sphere remains fixed. However, to the far sphere, an increase in (S/D) implies that both the influence of the near sphere and that of the plane decline. Therefore, for a fixed Re when (S/D) increases the decrease in the C_D for the far sphere is more pronounced than that for the near sphere. As in Fig. 3(a), C_D decreases with the increase in Re, and the more significant the boundary effect is the lower the value of Re at which the deviation from Stokes law occurs.

Figs. 4 and 5 show the variations of C_D as a function of (S/D) in a Newtonian fluid for various (h/r)s at two levels of Re. These figures reveal that, in general, C_D increases with the increase in (S/D) at the level of Re examined. Also, the more important the boundary effect (smaller h/r) the larger the C_D is. Note that for the far sphere, as (S/D) increases the $C_D - (h/r)$ curve should

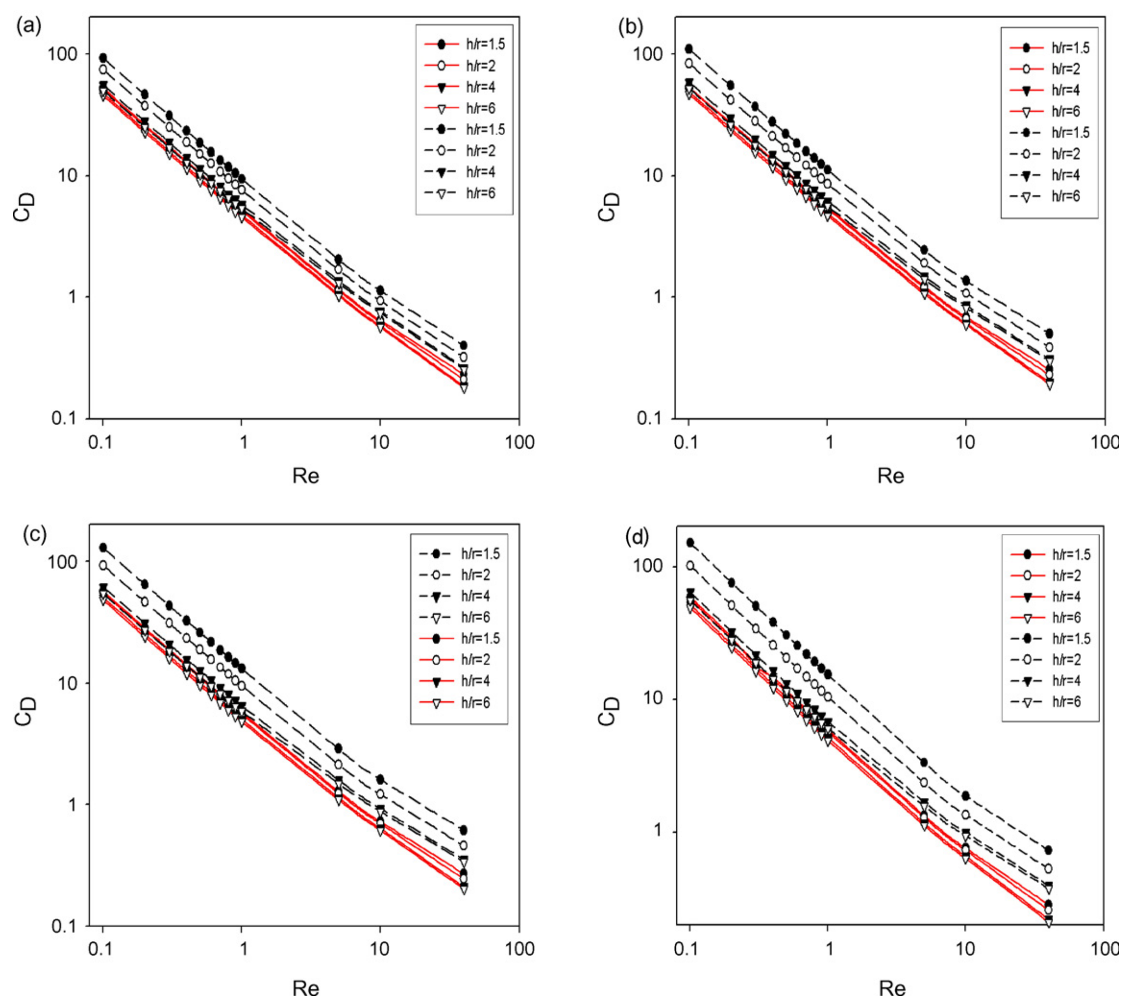

Fig. 7. Variation of C_D as a function of Re for various combinations of n and (h/r) at $Cu = 1$. (—): far sphere; (- - -): near sphere. (a) $n = 0.2$, (b) $n = 0.4$, (c) $n = 0.6$, (d) $n = 0.8$.

converge to a certain relation, as is seen in Fig. 4(a). The intersection of the $C_D-(h/r)$ curves at large (S/D) and small (h/r) arises from the limitation of the numerical method adopted, that is, it becomes less accurate under previous conditions. For a fixed value of (S/D), C_D approaches a constant value as (h/r) increases, implying that the boundary effect becomes negligible when the spheres are sufficiently far away from the plane. Here, we define a critical distance h_c for the near sphere beyond which the boundary effect can be neglected as following:

$$\frac{C_D(h_c/r)-C_D[(h_c+\Delta h)/r]}{(\Delta h/r)}\leq 3\% \tag{12}$$

where Δh is a small increment of h. The critical distance for the far sphere is $(h_c + S)$. The results of numerical simulation reveal that for the near sphere at a low Re, h_c declines with the increase in the separation distance between two spheres. For instance, if $Re = 0.1$, $h_c = 7.8r$ at $S/D = 1.5$, and $h_c = 7.1r$ at $S/D = 8$. As Re increases, the influence of the plane on the near sphere is lessened, and the critical distance decreases accordingly. For instance, if $Re = 40$, $h_c = 4.6r$ at $S/D = 1.5$ and $h_c = 4.0r$ at $S/D = 8$, but no general trend is observed when (S/D) varies. For the far sphere, regardless of the level of Re, h_c increases with the increase in (S/D). For example, if $Re = 0.1$, $h_c = 8.0r$ at $S/D = 1.5$, and $h_c = 10.1r$ at $S/D = 4$; if $Re = 40$, $h_c = 7.6r$ at $S/D = 1.5$, and $h_c = 12.4r$ at $S/D = 4$. Moreover, except for the case when $S/D = 1.5$, the value of h_c at a high level of Re is larger than that at a low level of Re. This might arise from that if two spheres are far apart, the near sphere and the plane can be viewed as another boundary to the far sphere, and this boundary has a prolonged influence on the far sphere. Letting C_{Dn} and C_{Df} be respectively the drag coefficient of the near sphere and that of the far sphere. For $Re \leq 1$, we obtain the following correlations:

$$C_{Dn}=\frac{1}{Re}\times\frac{3.8178+0.4325(S/D)-0.0334(S/D)^2}{1-1.4(r/h)+0.5(r/h)^2},\ Re\leq 1 \tag{13}$$

$$C_{Df}=C_{Dn}(1.62+0.048Re)(r/h)^{0.24},\ Re\leq 1 \tag{13a}$$

These relations are applicable to the ranges of the independent variables considered, and the maximum deviations of C_{Dn} and C_{Df} predicted by them are smaller than 5%. Some typical flow

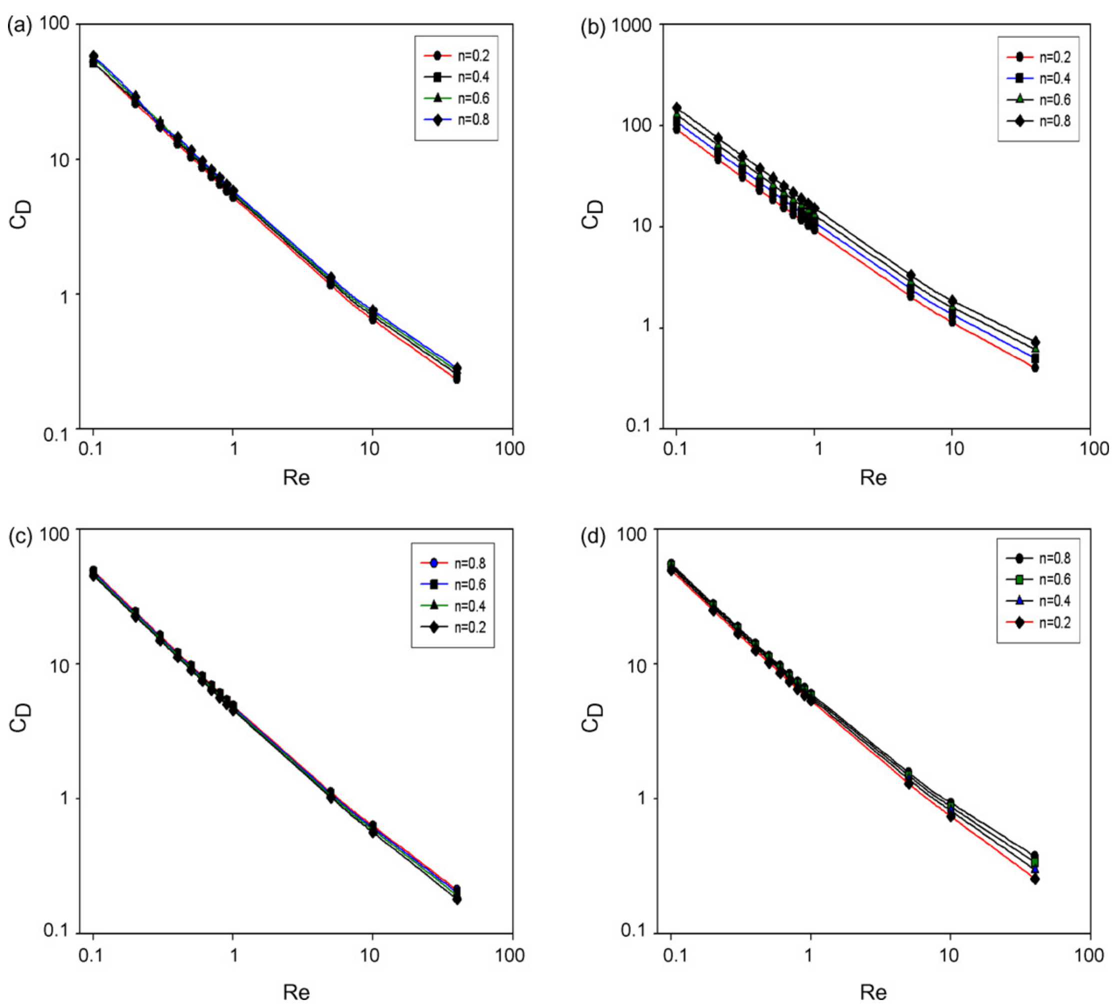

Fig. 8. Variation of C_D as a function of Re for various combinations of n and (h/r) at $Cu = 1$. (a) $h/r = 1.5$, far sphere, (b) $h/r = 1.5$, near sphere, (c) $h/r = 6$, far sphere, (d) $h/r = 6$, near sphere.

fields for the cases of Figs. 4 and 5 are illustrated in Fig. 6. Note that, as mentioned previously, we let both spheres be fixed in the space and the plane and the fluid move with a relative velocity u_t in the reverse direction. In general, the behaviors observed in Fig. 6 are consistent with the results shown in Figs. 4 and 5.

3.2. Carreau fluid

For the present Carreau fluid the Reynolds number *Re* and the Carreau number *Cu* are defined respectively by

$$Re = \frac{2\rho r u_t}{\eta_0} \tag{14}$$

$$Cu = \frac{\lambda u_t}{r} \tag{15}$$

Figs. 7 and 8 show the variation of the drag coefficient C_D as a function of *Re* for various combinations of *n* and (*h*/*r*). Here, the separation distance between two spheres and the value of *Cu* are fixed. The general trends of C_D as *Re* varies shown in Figs. 7 and 8 are similar to those for the case of a Newtonian fluid observed in Fig. 3. Quantitatively, the value of C_D for a Carreau fluid is smaller than that for the corresponding Newtonian fluid. Also, the degree of deviation of C_D from a Stokes-law like relation for a Carreau fluid is more serious than that for a Newtonian fluid. For a fixed value of *n* the closer the spheres to the plane the smaller the value of *Re* at which C_D starts to deviate from a Stokes-law like relation. If *n* is small, the shear-thinning nature of a Carreau fluid becomes important, its apparent viscosity is small, the fluid velocity is fast, the average *Re* is large, and therefore, C_D is smaller than that of the corresponding Newtonian fluid. If the boundary effect is unimportant, the shear-thinning nature of a Carreau fluid has the effect of reducing the influence of convective flow. On the other hand, if the boundary effect is important, that nature has the effect of enhancing the influence of convective flow. Therefore, if the spheres are close to the plane, the smaller the *n* the larger the amount of decrease in C_D, and the closer the corresponding C_D–*Re* curve to a Stokes-law like relation. On the other hand, if the spheres are far from the plane, it is easier for C_D to deviate from a Stokes-law like relation at a small value of *Re*.

The variations of the drag coefficient C_D as a function of *Re* at various combinations of *n* and (*S*/*D*) at $Cu = 1$ are illustrated in Figs. 9 and 10. Again, the qualitative behaviors of C_D are

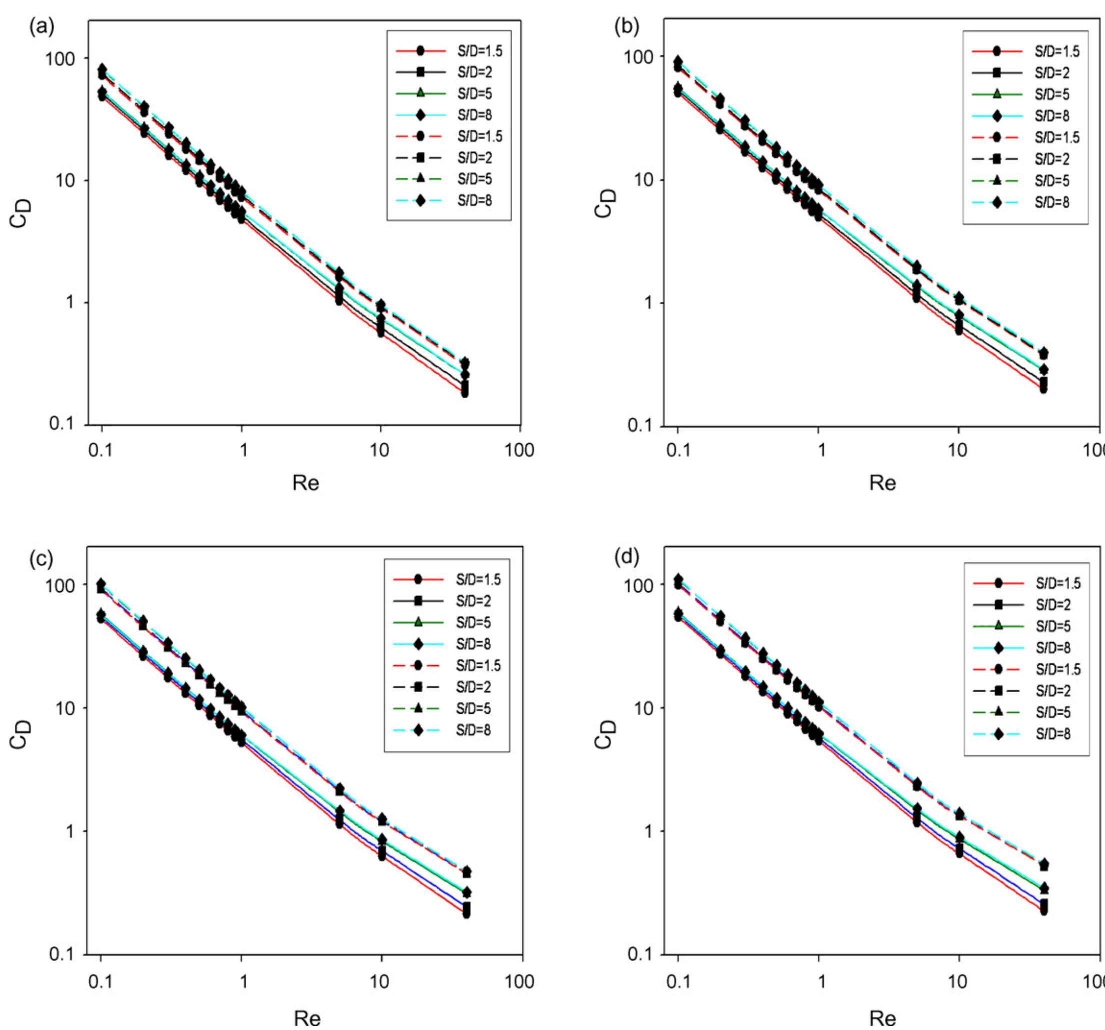

Fig. 9. Variation of C_D as a function of *Re* for various combinations of *n* and (*S*/*D*) at $h/r = 2$ and $Cu = 1$. (—): Far sphere; (- - -): near sphere. (a) $n = 0.2$, (b) $n = 0.4$, (c) $n = 0.6$, (d) $n = 0.8$.

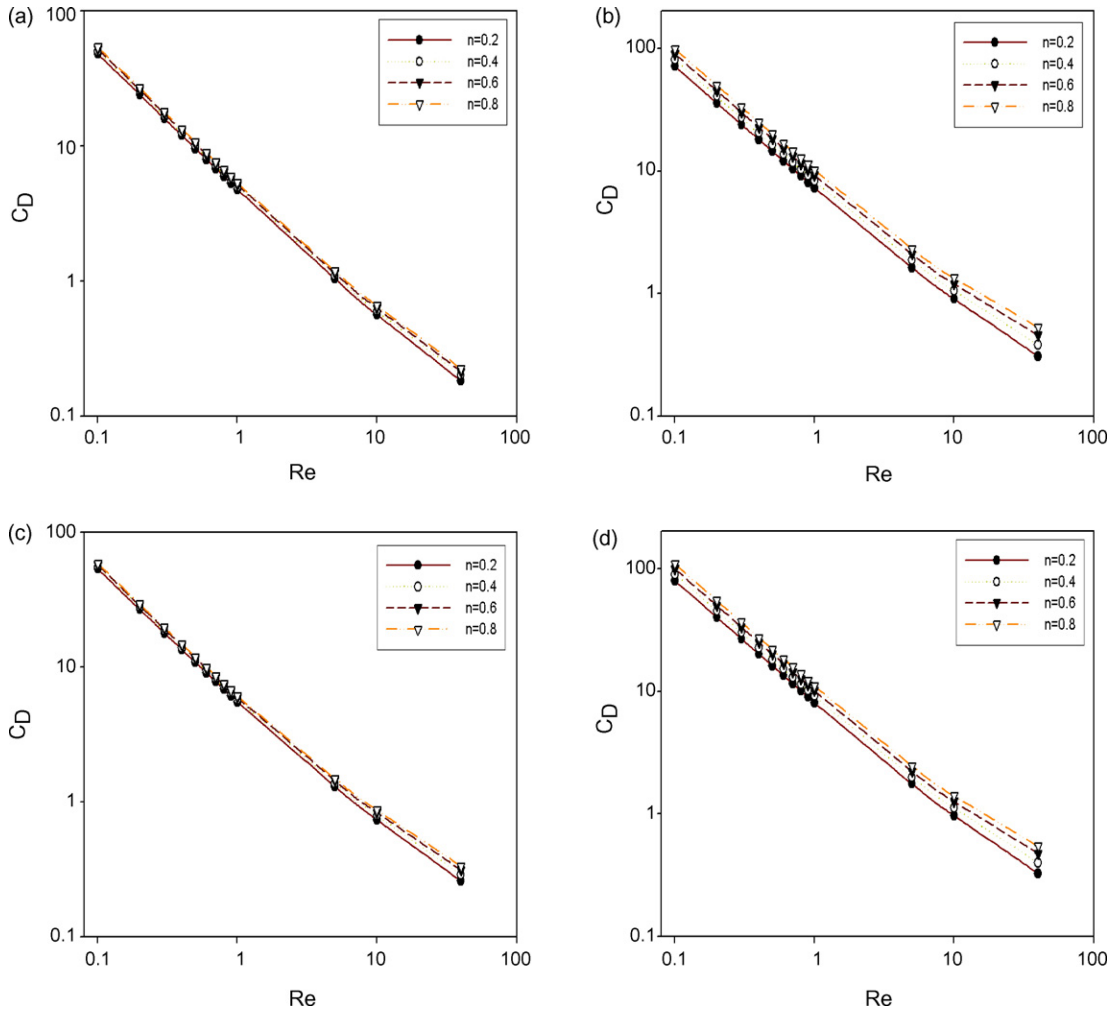

Fig. 10. Variation of C_D as a function of *Re* for various combinations of *n* and (*S*/*D*) at *h*/*r* = 2 and *Cu* = 1. (a) *S*/*D* = 1.5, far sphere, (b) *S*/*D* = 1.5, near sphere, (c) *S*/*D* = 5, far sphere, (d) *S*/*D* = 5, near sphere.

similar to those for a Newtonian fluid presented in Fig. 3, and the C_D for a Carreau fluid is smaller than that for the corresponding Newtonian fluid. The degree of deviation of the C_D–*Re* relation from Stokes law is more appreciable for the case of Carreau fluid. Also, the more significant the shear-thinning nature of a Carreau fluid is (e.g., smaller *n*) the smaller the *Re* at which the deviation from Stokes law occurs.

The variation of the drag coefficient of both spheres as a function of the separation distance between them (*S*/*D*) for various combinations of *n* and *Cu* at *h*/*r* = 2 and *Re* = 0.1 is presented in Fig. 11. This figure reveals that for the far sphere, as (*S*/*D*) increases C_D increases first and then decreases slightly, and for the near sphere, C_D increases with the increase in (*S*/*D*) and approaches a constant value. The larger the value of *n* the more appreciable these trends are. As expected, the larger the *Cu* and/or the smaller the *n*, that is, the more significant the shear-thinning nature of a Carreau fluid, the smaller the C_D. The influence of *n* on C_D is more appreciable when *Cu* is large.

Fig. 12 shows the variation of the drag coefficient of both spheres as a function of (*h*/*r*) for various combinations of *n* and *Cu* at *S*/*D* = 2 and *Re* = 0.1. This figure indicates that C_D declines with the increase in *Cu* and/or the decrease in *n*. These are expected since the more important the shear-thinning nature of a Carreau fluid the larger the *Re*. As can be seen in Fig. 11, if the spheres are close to the plane, because the presence of the latter has the effect of enhancing the shear-thinning nature of a Carreau fluid, the larger the *Cu* and/or the smaller the *n*, the more appreciable the decline of C_D. As *Cu* increases and/or *n* decreases, the influence of the plane on the behavior of the spheres declines. Also, C_D decreases with the increase in the separation distance between spheres and plane, and approaches a constant value, which is the result for the case when the plane is absent. If the influence of the plane is unimportant, the shear-thinning nature of a fluid has the effect of reducing the influence of convective flow; the reverse is true if it is important. The larger the value of *Cu* and/or the smaller the value of *n*, the smaller the variation of C_D as (*h*/*r*) increases. Furthermore, C_D increases with the increase in *n*, and the larger the value of *Cu* the more appreciable the influence of *n* on C_D. For the ranges of the parameters considered, h_c ranges from 4.0*r* to 7.7*r* for the near sphere and 6.0*r* to 8.5*r* for the far sphere. The more significant the shear-thinning nature of a Carreau fluid the smaller the value of h_c, that is, the boundary effect on C_D declines as *n* decreases and/or *Cu* increases. Similar to the case

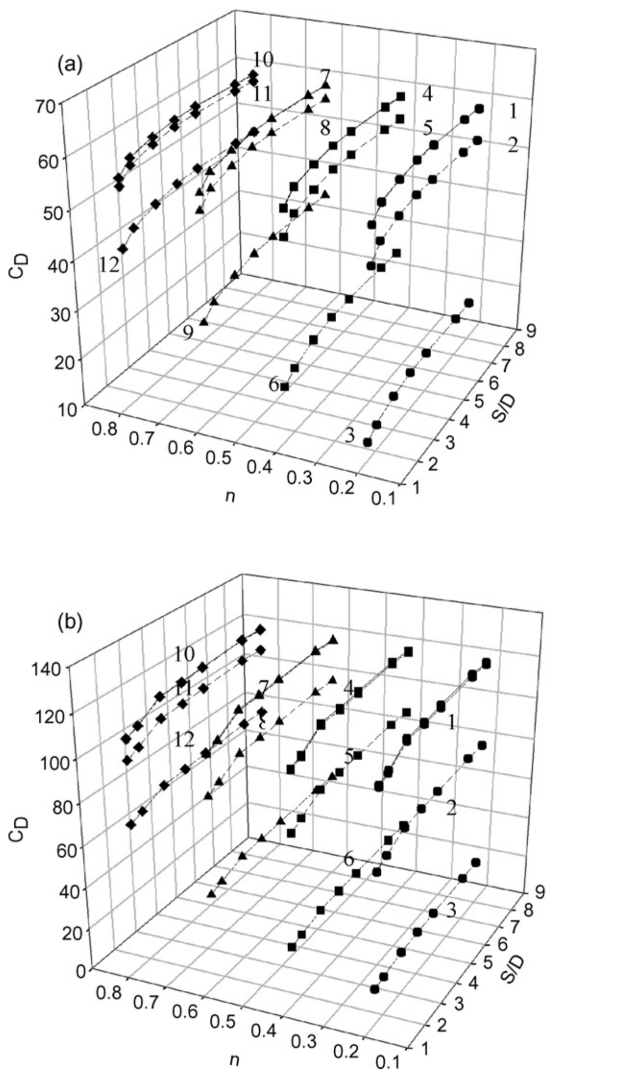

Fig. 11. Variation of C_D as a function of n and (S/D) for various Cus at Re = 0.1. (a) Far sphere, (b) near sphere. Curves 1, 4, 7, and 10, Cu = 0.1; curves 2, 5, 8, and 11, Cu = 1; curves 3, 6, 9, and 12, Cu = 10.

of C_D, the influence of n on h_c is appreciable when Cu is sufficiently large. As in the case of a Newtonian fluid, the value of h_c for the far sphere is larger than that for the near sphere, and can be explained by the same reasoning as that employed in the discussion of the results for a Newtonian fluid.

For $Re \leq 1$, the results obtained can be summarized by the correlations below:

$$C_{Dn} = \frac{1}{Re} \times \frac{1.9619 + 0.143(S/D) - 0.0117(S/D)^2}{(r/h)^{0.45} - 1.125(r/h)^{1.45} + 0.5(r/h)^{3.45}} \times [(1 + 0.21(n-1)Cu^{0.46})],\ Re \leq 1 \tag{16}$$

$$C_{Df} = C_{Dn}(1.955 + 0.066Re)(0.9237 + 0.4n)(r/h)^{0.41},\ Re \leq 1 \tag{16a}$$

These relations are applicable to the ranges of the independent variables considered, and the maximum deviations of C_{Dn} and C_{Df} predicted by these expressions are on the order of 10%.

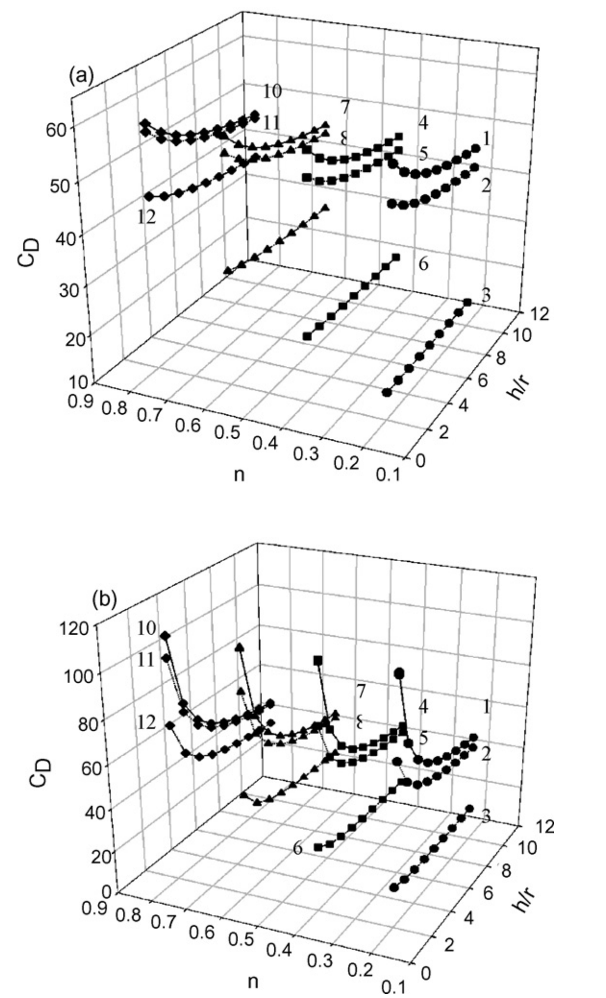

Fig. 12. Variation of C_D as a function of n and (h/r) for various Cus at Re = 0.1. (a) Far sphere, (b) near sphere. Curves 1, 4, 7, and 10, Cu = 0.1; curves 2, 5, 8, and 11, Cu = 1; curves 3, 6, 9, and 12, Cu=10.

Note that if Cu = 0 and/or n = 1, Eqs. (16) and (16a) do not reduce to Eqs. (13) and (13a), respectively, implying that there might exist several correlations of comparable performance.

4. Conclusion

The effects of the presence of a boundary and a nearby particle on the drag on a particle is investigated by considering two identical, co-axial, rigid spheres moving normal to a plane both in a Newtonian and in a Carreau fluid for a low to medium large Reynolds number. We show that the behaviors of the drag coefficient as the sphere-sphere distance and the sphere-boundary distance vary for the case of a Carreau fluid are similar to those for the case of a Newtonian fluid, except that the drag coefficient in the former is smaller than that in the latter. The influence of the boundary on the drag coefficient is more appreciable than that of the fluid nature. The influence of the index parameter of a Carreau fluid on the drag coefficient is insensitive to the level of Reynolds number; that influence becomes appreciable only if the Carreau number is sufficiently large. Regardless of the level of the Reynolds number, the critical separation distance, the sphere-boundary distance beyond which the boundary effect is unimportant, of the far sphere declines with the increase in the separation distance between two spheres. For the near sphere at a low Reynolds number, the critical separation distance increases with the increase in the separation distance between two spheres. For both spheres, the more significant the shear-thinning nature of a Carreau fluid, the shorter the critical separation distance is.

Acknowledgement

This work is supported by the National Science Council of the Republic of China.

References

Adachi, K., N. Yoshioka, and K. Yamamoto, "On Non-Newtonian Flow Past a Sphere," *Chem. Eng. Sci.*, **28**, 2033 (1973).

Becker, L. E., G. H. McKinley, and H. A. Stone, "Sedimentation of a Sphere near a Plane Wall: Weak Non-Newtonian and Inertial Effects," *J. Non-Newtonian Fluid Mech.*, **63**, 201 (1996).

Ceylan, K., S. Herdem, and T. Abbasov, "A Theoretical Model for Estimation of Drag Force in the Flow of Non-Newtonian Fluids around Spherical Solid Particles," *Powder Technol.*, **103**, 286 (1999).

Chhabra, R. P. and P. H. T. Uhlherr, "Sphere Motion through Non-Newtonian Fluids at High Reynolds Number," *Can. J. Chem. Eng.*, **58**, 124 (1980).

Happel, J. and H. Brenner, *Low Reynolds Number Hydrodynamics*, Academic Press, New York, U.S.A, p. 330.

Kelessidis, V. C. and G. Mpandelis, "Measurements and Prediction of Terminal Velocity of Solid Spheres Falling through Stagnant Pseudoplastic Liquids," *Powder Technol.*, **147**, 117 (2004).

Machač, I., B. Šiška, and L. Machačcvá, "Terminal Falling Velocity of Spherical Particles Moving through a Carreau Model Fluid," *Chem. Eng. Proc.*, **39**, 365 (2000).

Machač, I., B. Šiška, and R. Teichman, "Fall of Non-Spherical Particles in a Carreau Model Liquid," *Chem. Eng. Proc.*, **41**, 577 (2002).

Missirlis, K. A., D. Assimacopoulos, E. Mitsoulis, and R. P. Chhabra, "Wall Effects for Motion of Spheres in Power-Law Fluids," *J. Non-Newtonian Fluid Mech.*, **96**, 459 (2001).

Rodrigue, D., D. De Kee, and C. F. Chan Man Fong, "The Slow Motion of a Spherical Particle in a Carreau Fluid," *Chem. Eng. Commun.*, **154**, 203 (1996).

Tripathi, A. and R. P. Chhabra, "Drag on Spheroidal Particles in Dilatant Fluids," *AIChE J.*, **41**, 728 (1995).

兩共軸剛性球在一牛頓及卡羅流體中垂直於一平板運動時所受之拖曳力

徐治平　楊淑娟　陳榮傑
國立台灣大學化學工程學系

摘　要

藉著考慮兩相同之共軸剛性球在一牛頓及卡羅流體中垂直於一平板的運動，吾人探討了邊界效應與周邊粒子，在中及低雷諾數下，對一粒子沉降時所受拖曳力之影響。文中討論了系統之主要參數，包括流體特性、兩球間距離、較近球與平板間距離、與雷諾數等，與拖曳係數間的關係。數值模擬的結果顯示，邊界效應對拖曳係數的影響較流體特性與兩球間距離者為重要。卡羅流體中拖曳係數隨雷諾數變化的關係與牛頓流體中者類似，但前者中的剪致變稀特性有降低拖曳係數之效應。卡羅數夠大時，卡羅流體之指數參數的影響始較顯著。在雷諾數小於 1 的情況下，吾人獲得了拖曳係數與系統主要參數間的相關式。